Research Article

Maolin Ye, Xiaojun Xi, Shufeng Yang*, Jingshe Li, and Feng Wang

# Dephosphorization of hot metal using rare earth oxide-containing slags

https://doi.org/10.1515/htmp-2020-0090
received September 10, 2018; accepted December 26, 2018

**Abstract:** An innovative rare earth oxide-containing slag for hot metal dephosphorization was proposed, and the factors influencing the efficiency during the dephosphorization of hot metal using rare earth oxide-containing slags were also studied. An increase in the temperature up to 1,550°C is beneficial to the dephosphorization process, and the maximum degree of dephosphorization for slags containing 6 wt% rare earth oxides is 44.49%; further temperature increases would deteriorate the efficiency, and the degree of dephosphorization decreases to 37.38% at 1,600°C. An increase in the basicity of slags up to 3.0, and the rare earth oxide content up to 6 wt%, improves the dephosphorization efficiency; further increase in the basicity and rare earth oxide content, the efficiency has almost no change. It was also found that an increase in the quantity of slags is beneficial to the dephosphorization reaction.

**Keywords:** hot metal dephosphorization, rare earth oxide-containing slags, double-layer graphite crucible

## 1 Introduction

Phosphorus is considered detrimental to most of the steel grades. A high phosphorus content in steel materials would lead to low ductility and poor mechanical properties as well as welding performance. Therefore, the development of highly efficient dephosphorization technologies for high phosphorus content hot metal has been attracting significant interest [1].

There are several slags used to remove phosphorus under oxidizing conditions. CaO-Based slags were widely used for dephosphorization of hot metal because of their low price [2]. However, CaO-based slags have a high melting point, and lower temperatures thermodynamically aid in the dephosphorization reaction. Therefore, $CaF_2$ and other fluxes are usually added to the molten slag to decrease its melting point and to enhance the kinetics of the dephosphorization process [3,4]. The melting properties of $CaO–Fe_2O_3–Na_2O–Al_2O_3–CaF_2$ dephosphorization slag were measured using the hemisphere method. The results showed that both $Al_2O_3$ and $Na_2O$ are beneficial to the slag melted and dephosphorization process [5]. Pak and Fruehan [6] indicated that the addition of small amounts of $Na_2O$ to CaO-based slags greatly improved the dephosphorization rate. Jung et al. [7] reported that an increase in the MnO contents causes an increase in the phosphorus distribution ratio between $CaO–SiO_2–MgO–Al_2O_3–Fe_tO–MnO–P_2O_5$ slag and hot metal. Gao et al. [8] and Matsuura et al. [9] studied the phase equilibrium for the $CaO–SiO_2–FeO–P_2O_5–Al_2O_3$ system for the dephosphorization of hot metal pretreatment at different experimental conditions. The results showed that the solid solution combined with $2CaO·SiO_2$ and $3CaO·P_2O_5$ easily forms under the dephosphorization conditions, which indicates the possibility of using the solid phase in the multiphase flux system to absorb phosphorus from the liquid slag.

The most common type of rare earth (RE) phosphate mineral is Monazite, which contains Ce, La, Nd and Th $[PO_4]$. This indicates that the RE phosphate is very stable and suggests that its activity in the molten slag is low. On the other hand, the optical basicity values of $Ce_2O_3$ and $La_2O_3$ are higher than those of CaO and BaO, the optical basicity values of CaO and BaO are 1.0 and 1.15 [10,11], but the optical basicity values of $Ce_2O_3$ and $La_2O_3$ reach 1.23 and 1.18 [12,13], respectively. Based on these conditions, Xi et al. [14] studied the phosphorus

* **Corresponding author: Shufeng Yang,** School of Metallurgical and Ecological Engineering, University of Science and Technology Beijing, Beijing, 100083, China; Beijing Key Laboratory of Special Melting and Preparation of High-End Metal Materials, Beijing, 100083, China, e-mail: yangshufeng@ustb.edu.cn
**Maolin Ye, Xiaojun Xi, Jingshe Li, Feng Wang:** School of Metallurgical and Ecological Engineering, University of Science and Technology Beijing, Beijing, 100083, China; Beijing Key Laboratory of Special Melting and Preparation of High-End Metal Materials, Beijing, 100083, China

distribution between $CaO–SiO_2–MnO–Ce_2O_3–La_2O_3$ slags and ferromanganese alloy, and the results showed that an increase in the RE oxide content in molten slags improves the phosphorus distribution ratio. However, RE oxides have a limited solubility in molten slags [15], while excessive RE oxides in the slags cause an increase in the molten temperature and viscosity, thus deteriorating the dephosphorization kinetics [16].

This article proposes the partial substitution of CaO with $Ce_2O_3$ and $La_2O_3$ in the dephosphorization slags, and a systematic research on the factors affecting the dephosphorization efficiency is also reported.

## 2 Experiments

The basicity (binary basicity, wt% CaO/wt% $SiO_2$, the same as below) of the intended slags was set at 2.0, 2.5, 3.0 and 3.5. Contents of rare earth oxides were fixed at 0, 2, 4, 6, 8 and 10 wt%. The slags were prepared by mixing reagent-grade CaO, $SiO_2$, $Fe_2O_3$, $La_2O_3$ and $CeO_2$. $CeO_2$ was used instead of $Ce_2O_3$ because in the operating conditions of the steelmaking process, cerium oxides exist mainly in the form of $Ce_2O_3$ [17]. The required amounts of the slag components were dried, weighted and mixed homogeneously in an agate mortar. The chemical compositions of the designed slag samples are shown in Table 1.

The metal samples were prepared by using pure iron (Fe ≥ 99.9 wt%) and ferro-phosphorus (P-24.15 wt%). In order to prevent the graphite crucibles from being eroded by hot metal, 4 wt% of carbon powder was added to the metal samples. The required amount of the metal components was weighted, mixed homogeneously and placed at the bottom of graphite crucibles (60 mm in diameter, 120 mm in height). The samples were melted by a non-oxidation process in a high-temperature electric pipe furnace with an $MoSi_2$ heating element (Tianjin Taisite Instrument Co., Ltd, China). The metal phase was analysed by inductively coupled plasma (ICP) method for P content. The result showed that the P content of metal phase was 0.436 wt%.

Dephosphorization process is significantly influenced by temperature. The thermodynamic analysis indicates that a lower temperature favours dephosphorization under oxidizing conditions [18], but the reaction rates are relatively low, whereas a higher temperature will tend to improve the dephosphorization kinetics. To ensure that the metal sample in the graphite crucible was completely melted, a preliminary experiment was carried out to determine the melting process of the metal sample. The result showed that the metal sample was completely melted at approximately 1,450°C. Therefore, all the dephosphorization experiments were carried out above 1,450°C.

The dephosphorization experiments were performed using a high-temperature electric pipe furnace with an alumina work tube. The dephosphorization reaction was carried out in double-layer graphite crucibles using molten slag dropping into molten iron, as shown in Figure 1. The upper graphite crucible (80 mm in diameter, 20 mm in height) with a small hole at the bottom, the small hole inserted using one graphite stopper rod, was loaded with mixed slag. The lower graphite crucible (80 mm in diameter, 50 mm in height) was filled with approximately $400 \times 10^{-3}$ kg of the metal sample. The double-layer graphite crucibles were placed in the even temperature zone of the furnace and were heated to the predetermined experimental temperature at a rate of 10°C/min under the protection of high-purity argon gas. It was then held at this temperature for 20 min to homogenize the sample. The graphite stopper

**Table 1:** Chemical composition of designed slags (wt%)

| Slag no. | $CaO/SiO_2$ | CaO | $SiO_2$ | $Fe_2O_3$ | $La_2O_3$ | $CeO_2$ |
|---|---|---|---|---|---|---|
| 1 | 2.0 | 54.27 | 26.89 | 12.51 | 3.0 | 3.0 |
| 2 | 2.5 | 58.04 | 23.21 | 12.63 | 3.0 | 3.0 |
| 3 | 3.0 | 64.68 | 21.51 | 13.78 | 0 | 0 |
| 4 | 3.0 | 63.28 | 21.06 | 13.56 | 1.0 | 1.0 |
| 5 | 3.0 | 62.27 | 20.66 | 13.04 | 2.0 | 2.0 |
| 6 | 3.0 | 60.89 | 20.28 | 12.55 | 3.0 | 3.0 |
| 7 | 3.0 | 59.88 | 19.85 | 11.95 | 4.0 | 4.0 |
| 8 | 3.0 | 59.17 | 19.59 | 11.12 | 5.0 | 5.0 |
| 9 | 3.5 | 63.18 | 17.95 | 12.69 | 3.0 | 3.0 |

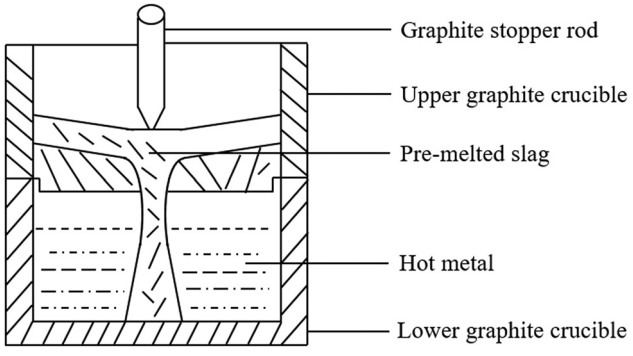


**Figure 1:** Schematic diagram of dephosphorization test with double-layer graphite crucibles.

rod was then taken away and the molten slag was poured into the hot metal, at which point, time recording started. The dephosphorization time for each run was 16 min, which had been found to be sufficient in previous research [19]. After dephosphorization equilibration, the graphite crucible containing the reacted samples was taken out of the reaction tube and quenched in water. After quenching, the samples were taken out of the crucibles and separated into the slag and metal phases, which were then ground into powder. The metal phases were analysed by ICP atomic emission spectroscopy method for their Fe and P contents. The slag phases were analysed by X-ray fluorescence for $Fe_2O_3$, $La_2O_3$, $Ce_2O_3$ and $P_2O_5$ contents.

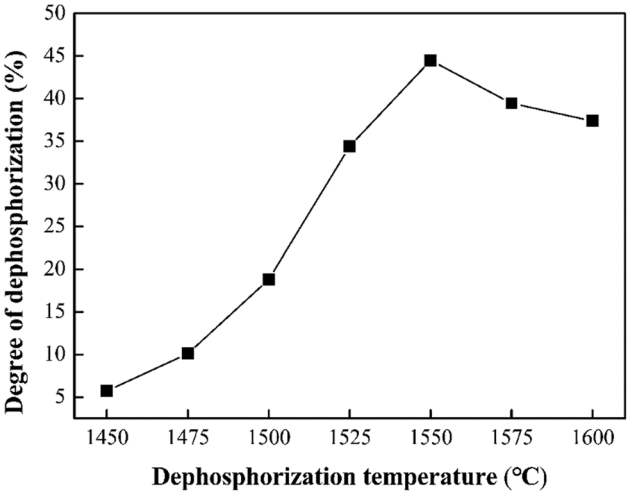


**Figure 2:** Relationship between dephosphorization efficiency and temperature.

# 3 Results and discussion

The following parameters were varied to evaluate their effect on the dephosphorization efficiency: (i) rare earth oxide contents in dephosphorization slags, (ii) basicity, (iii) temperature and (iv) quantity of dephosphorization slags.

## 3.1 Dephosphorization temperature

Dephosphorization slag No. 6 and metal sample were used to investigate the effect of temperature on the dephosphorization efficiency. The contents of different components in slag and metal sample after dephosphorization experiment are listed in Table 2.

The data in Figure 2 indicate that the degree of dephosphorization initially increased as the temperature increased up to 1,550°C, and then the dephosphorization efficiency decreased as the temperature increased above 1,550°C.

The chemical equation of hot metal dephosphorization using rare earth oxide-containing slags is expressed by the ion theory according to equation (1)

$$\frac{1}{2}P_2(g) + \frac{5}{4}O_2(g) + \frac{3}{2}(O^{2-}) = (PO_4^{3-}) \quad (1)$$

$$K_1 = \frac{\alpha_{PO_4^{3-}}}{P_{P_2}^{1/2} \cdot P_{O_2}^{5/4} \cdot \alpha_{(O^{2-})}^{3/2}} \quad (2)$$

where $\alpha_i$, $P_i$ and $K_1$ are the activity of $i$, the partial pressure of $i$ and equilibrium constant of equation (1), respectively.

The phosphate capacity $C_{PO_4^{3-}}$ of the rare earth oxide-containing slags can be defined by equation (3).

$$C_{PO_4^{3-}} = \frac{(\text{wt\% } PO_4^{3-})}{P_{P_2}^{1/2} \cdot P_{O_2}^{5/4}} = \frac{K_1 \cdot \alpha_{O^{2-}}^{3/2}}{\gamma_{PO_4^{3-}}} \quad (3)$$

where $\gamma_{PO_4^{3-}}$ is the activity coefficient of $PO_4^{3-}$.

According to the equilibrium constant $K_1$ of the dephosphorization reaction and Van't Hoff's equation (4),

**Table 2:** Chemical composition of slags and metal after dephosphorization experiments at different temperatures (wt%)

| Slag no. | Temp. (°C) | Slag and metal samples' composition (wt%) | | | | | | Degree of dephos. (%) |
|---|---|---|---|---|---|---|---|---|
| | | (FeO) | ($La_2O_3$) | ($Ce_2O_3$) | ($P_2O_5$) | [Fe] | [P] | |
| 6 | 1,450 | 27.89 | 2.94 | 1.93 | 0.06 | 98.78 | 0.411 | 5.73 |
| | 1,475 | 27.91 | 2.91 | 1.86 | 0.11 | 98.69 | 0.392 | 10.10 |
| | 1,500 | 27.12 | 3.07 | 1.92 | 0.19 | 99.04 | 0.354 | 18.81 |
| | 1,525 | 28.39 | 2.85 | 1.98 | 0.35 | 97.85 | 0.286 | 34.40 |
| | 1,550 | 27.85 | 2.77 | 1.87 | 0.45 | 98.82 | 0.242 | 44.49 |
| | 1,575 | 28.09 | 2.98 | 1.91 | 0.40 | 98.63 | 0.264 | 39.45 |
| | 1,600 | 27.98 | 2.86 | 1.92 | 0.38 | 98.75 | 0.273 | 37.38 |

the relation between phosphate capacity of the rare earth oxide-containing slags and temperature can be expressed as equations (5) and (6).

$$\frac{\partial \ln K_1}{\partial T} = \frac{\Delta H_1}{RT^2} \tag{4}$$

$$\frac{\partial \ln [C_{PO_4^{3-}} \cdot \gamma_{PO_4^{3-}} \cdot \gamma_{O^{2-}}^{-3/2}]}{\partial(1/T)} = -\frac{\Delta H_1}{R} \tag{5}$$

$$\Delta H_1 = \Delta H_1^{\theta} + \Delta H_{PO_4^{3-}} - \frac{3}{2}\Delta H_{O^{2-}} \tag{6}$$

where $\Delta H_1$ is the heat change for the dephosphorization reaction using rare earth oxide-containing slags; $\Delta H_1^{\theta}$ is the heat change of dephosphorization reaction (1) when using pure substances; $R$ is constant; $\gamma_{O^{2-}}$ is the activity coefficient of $O^{2-}$; $\Delta H_{PO_4^{3-}}$ and $\Delta H_{O^{2-}}$ are the partial molar heats of solution of $PO_4^{3-}$ and $O^{2-}$ in molten slags. Neglecting the influence of temperature on the activity coefficients of $PO_4^{3-}$ and $O^{2-}$, then equation (5) can be simplified as equation (7).

$$\frac{\mathrm{d} \lg C_{PO_4^{3-}}}{\mathrm{d}(1/T)} = -\frac{\Delta H_1}{2.303R} \tag{7}$$

Ferromanganese dephosphorization is an exothermic reaction, and an increase in the dephosphorization temperature causes a decrease in the phosphate capacity of rare earth oxide-containing slags, as shown in equation (7). The thermodynamic analysis indicates that a lower temperature favours dephosphorization under oxidizing condition. However, dephosphorization process is a liquid phase reaction, controlled by material diffusion in the liquid phase and interface chemical reaction. A lower temperature leads to an uneven melting of the slag, and the transfer of material is rate-limiting, which leads to a poor kinetics of dephosphorization [16]. Therefore, when the temperature is below 1,550°C, the dephosphorization efficiency is mainly influenced by the kinetics, and an increase in temperature up to 1,550°C causes an increase in dephosphorization efficiency. However, when the temperature increase is above 1,550°C, the effect of kinetics on dephosphorization can be neglected, and thermodynamic limitations cause a drop in the dephosphorization efficiency.

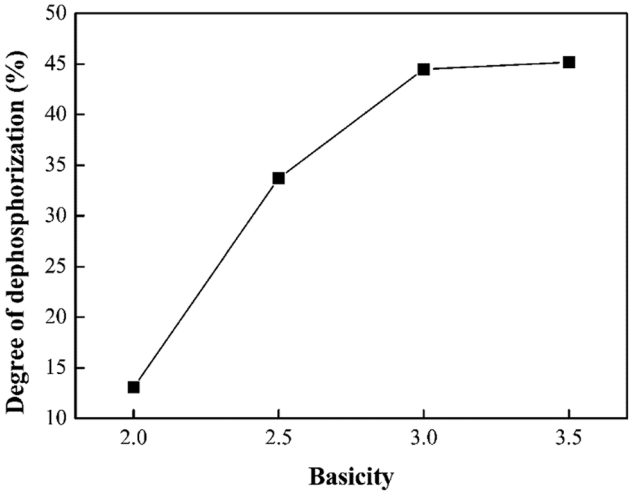


**Figure 3:** Relationship between dephosphorization efficiency and basicity.

## 3.2 Basicity

Dephosphorization slags Nos. 1, 2, 6 and 9 and metal sample were employed to study the effect of basicity on the dephosphorization efficiency. The contents of different components in slag and metal sample after dephosphorization experiment are listed in Table 3. As shown in Figure 3, the degree of dephosphorization initially increased as the basicity of slag increased up to 3.0, and the degree of dephosphorization has almost no change when the basicity is further increased to 3.5.

With the increase of basicity, the effective solubility of CaO in the slags increases. According to the slag ion structure theory, CaO is alkaline oxide, which can provide free oxygen ions ($O^{2-}$) into the dephosphorization slags [20]. The free oxygen ions ($O^{2-}$) in slags increase as the basicity increases. As shown in equation (1), an increase in the $O^{2-}$ contents facilitates the

**Table 3:** Chemical composition of slags and metal after dephosphorization experiments at 1,550°C (wt%)

| Slag no. | Basicity | Slag and metal samples' composition (wt%) | | | | | | Degree of dephos. (%) |
|---|---|---|---|---|---|---|---|---|
| | | (FeO) | ($La_2O_3$) | ($Ce_2O_3$) | ($P_2O_5$) | [Fe] | [P] | |
| 1 | 2.0 | 29.12 | 2.93 | 1.84 | 0.14 | 96.97 | 0.379 | 13.07 |
| 2 | 2.5 | 27.96 | 2.81 | 1.79 | 0.34 | 98.85 | 0.289 | 33.72 |
| 6 | 3.0 | 27.85 | 2.77 | 1.87 | 0.45 | 98.82 | 0.242 | 44.49 |
| 9 | 3.5 | 28.04 | 2.83 | 1.92 | 0.45 | 98.77 | 0.239 | 45.18 |

dephosphorization reaction. In addition, dephosphorization product ($P_2O_5$) is acid oxide, so an increase in the basicity of dephosphorization slags is beneficial to dilute the concentration of $P_2O_5$, thus improving the degree of dephosphorization [14].

The dephosphorization efficiency is also affected by the kinetics factor. When the basicity of slags is below 3.0, an increase in the basicity of slags causes an increase in $O^{2-}$. $O^{2-}$ can depolymerize the complicated network structure of the silica complex ions [21]. In addition, an increase in the $O^{2-}$ contents will lead to an increase in the molar ratio between oxygen and silicon (OSI), and the complicated network structure of the silica complex ions is gradually transformed from skeleton (OSI = 2.0), to lamellar (OSI = 2.5), to chain (OSI = 3.0) and finally to Volmer–Weber (OSI = 4.0). Throughout these transformations, the viscous activation energy and viscosity of the slags decrease [22]. A decrease in viscosity of the slags is beneficial to melt evenly, thus improving the dephosphorization efficiency. However, when the basicity of slags is increased to 3.5, the viscosity of the slags increases, thermodynamic and kinetic effects balance out and the degree of dephosphorization has almost no change.

## 3.3 Rare earth oxide contents in dephosphorization slags

Dephosphorization slags No. 3 to 8 and metal sample were used to study the effect of basicity on the dephosphorization efficiency. The contents of different components in slag and metal sample after dephosphorization experiment are listed in Table 4. For dephosphorization slags with a basicity of 3.0, the degree of dephosphorization increases from 7.57% to 50.45% as the rare earth oxide contents increase from 0 to 10 wt%, and when the rare earth oxide contents increase above 6 wt%, the increasing trend gradually decreases, as shown in Figure 4.

Optical basicity is a concept that provides a good foundation for a better understanding of the behaviour of molten slags than the conventional basicity ratio [11,12]. The optical basicity value for the oxide can be calculated by equation (8) [23].

$$\Lambda_i = \frac{0.74}{X - 0.26} \tag{8}$$

where $\Lambda_i$ is the optical basicity of each oxide and $X$ is the Pauling electronegativity of the cation.

The optical basicity of a multicomponent dephosphorization slag can be calculated by equations (9) and (10).

$$\Lambda = \sum \Lambda_i N_i \tag{9}$$

$$N_i = \frac{x_i n_{O_i}}{\sum_{j=1}^{n} x_i n_{O_i}} \tag{10}$$

where $N_i$ is the equivalent cation fraction of each oxide; $x_i$ is the mole fraction of $i$ component; and $n_{O_i}$ is the number of oxygen atoms in the $i$ components of the molten slag.

The optical basicity value of CaO is 1.0, but the optical basicity values of $Ce_2O_3$ and $La_2O_3$ reach 1.23 and 1.18. According to equations (9) and (10), the partial substitution of CaO with $Ce_2O_3$ and $La_2O_3$ can improve the optical basicity values of dephosphorization slags. Yang et al. [23] reported that an increase in the optical basicity values causes an increase in the phosphate capacity of dephosphorization slags. Therefore, an increase in the rare earth oxide contents in dephosphorization slags causes an increase in the optical basicity values, thus improving the dephosphorization efficiency. In addition, rare earth oxides dissolved in molten slags can ionize a large amount of $O^{2-}$ and depolymerize the complicated network structure of the silica complex ions, thus improving the fluidity of the slags [21]. The slag with good fluidity is beneficial to the dephosphorization material diffusion and improves the interface chemical reaction. Therefore, an increase in the mass fraction of rare earth oxides in the molten slags

**Table 4:** Chemical composition of slags and metal after dephosphorization experiments at 1,550°C (wt%)

| Slag no. | Slag and metal samples' composition (wt%) | | | | | | Degree of dephos. (%) |
|---|---|---|---|---|---|---|---|
| | (FeO) | ($La_2O_3$) | ($Ce_2O_3$) | ($P_2O_5$) | [Fe] | [P] | |
| 3 | 29.04 | 0 | 0 | 0.07 | 97.93 | 0.403 | 7.57 |
| 4 | 28.25 | 0.92 | 0.58 | 0.21 | 98.15 | 0.345 | 20.87 |
| 5 | 27.69 | 1.84 | 1.25 | 0.34 | 98.94 | 0.287 | 34.17 |
| 6 | 27.85 | 2.77 | 1.87 | 0.45 | 98.82 | 0.242 | 44.49 |
| 7 | 27.99 | 3.70 | 2.49 | 0.48 | 98.66 | 0.225 | 48.39 |
| 8 | 27.89 | 4.61 | 3.12 | 0.50 | 98.75 | 0.216 | 50.45 |

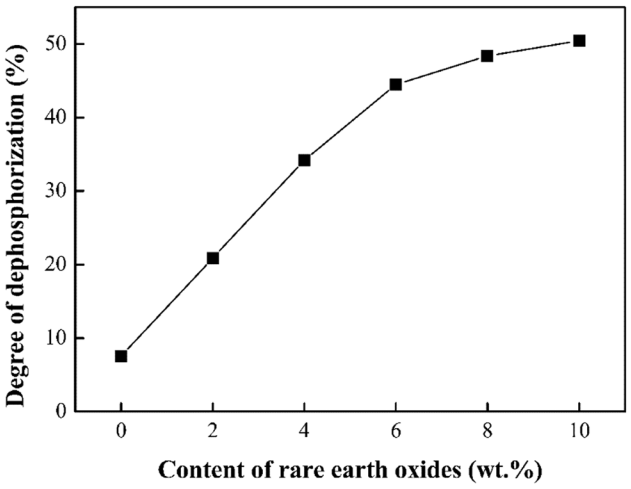


**Figure 4:** Relationship between dephosphorization efficiency and rare earth oxide content.

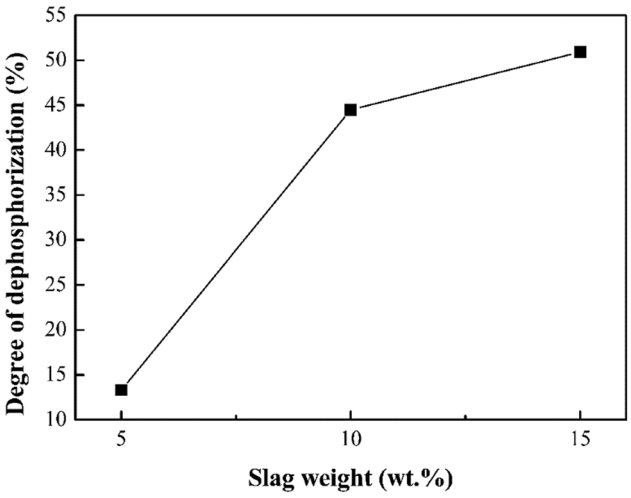


**Figure 5:** Relationship between dephosphorization efficiency and quantity of slags.

causes an increase in the dephosphorization efficiency. However, rare earth oxides have a limited solubility in molten slags [15]. When the mass fraction of rare earth oxides increases above 6 wt%, their solubility decreases, leading to a poor fluidity of the slags; thus, the thermodynamic and kinetic effects balance out and the dephosphorization efficiency changes little.

## 3.4 Quantity of dephosphorization slags

This study used dephosphorization slag No. 6 and metal sample to investigate the effect of the quantity of slags on the dephosphorization efficiency at 1,550°C. The mass fractions of dephosphorization slags were 5, 10 and 15 wt%. The contents of different components in slag and metal after experiment are listed in Table 5. An increase in the amount of dephosphorization slag is beneficial to the dephosphorization reaction, as shown in Figure 5. When the quantity of slags increases from 5 to 15 wt%, the degree of dephosphorization increases from 13.30 to 50.92%.

Due to the pure iron and ferro-phosphorus inevitably containing silicon, the affinity of Si with O is much stronger than that of P. Therefore, Si oxidation consumes a portion of the dephosphorization slag and the product of the Si oxidation reaction decreases the basicity of the dephosphorization slag [14]. However, an increase in the quantity of dephosphorization slags can meet the amount of slag required for dephosphorization, thus increasing the dephosphorization efficiency. In addition, an increase in the amount of dephosphorization slag is beneficial to dilute the concentration of $P_2O_5$ and decrease the content of phosphate in slag [14]. Therefore, the dephosphorization efficiency increases with increasing the quantity of dephosphorization slags.

# 4 Conclusions

(1) When the dephosphorization temperature is lower than 1,550°C, the dephosphorization process is mainly influenced by the kinetic factors, and the dephosphorization efficiency increases, as the

**Table 5:** Chemical composition of slags and metal after dephosphorization experiments at 1,550°C (wt%)

| Slag no. | Slag weight (%) | Slag and metal samples' composition (wt%) | | | | | | Degree of dephos. (%) |
|---|---|---|---|---|---|---|---|---|
| | | (FeO) | ($La_2O_3$) | ($Ce_2O_3$) | ($P_2O_5$) | [Fe] | [P] | |
| 6 | 5 | 27.66 | 2.86 | 1.76 | 0.14 | 98.63 | 0.378 | 13.30 |
| | 10 | 27.85 | 2.77 | 1.87 | 0.45 | 98.82 | 0.242 | 44.49 |
| | 15 | 29.35 | 2.64 | 1.75 | 0.51 | 96.85 | 0.214 | 50.92 |

temperature increases below 1,550°C. When the temperature increases above 1,550°C, the thermodynamic limitations cause an obvious drop in dephosphorization efficiency.

(2) An increase in both the basicity of slags and the rare earth oxide content in slags is beneficial to dephosphorization process. However, when the basicity of slags increases above 3.0, and the content of rare earth oxides in slags reaches more than 6 wt%, the dephosphorization efficiency has almost no change.

(3) An increase in the amount of dephosphorization slag is beneficial to the dephosphorization reaction, but excessive slag will cause an increase in Fe loss.

**Acknowledgments:** The authors gratefully acknowledge the support by the National Natural Science Foundation of China (NSFC, Nos. 51734003 and 51874116).

**Conflict of interest:** The authors declare no conflict of interest.

# References

[1] Tian, Z. H., B. H. Li, X. M. Zhang, and Z. H. Jiang. Double slag operation dephosphorization in BOF for producing low phosphorus steel. *Journal of Iron and Steel Research International*, Vol. 16, 2009, pp. 6–14.

[2] Ito, K., and M. Terasawa. Utilization of multiphase fluxes for the dephosphorization of hot metal. *Steel Research International*, Vol. 80, 2010, pp. 733–736.

[3] Li, F. S., X. P. Li, S. F. Yang, and Y. L. Zhang. Distribution ratios of phosphorus between CaO-FeO-$SiO_2$-$Al_2O_3$/$Na_2O$/$TiO_2$ slags and carbon-saturated iron. *Metallurgical and Materials Transactions B*, Vol. 48, 2017, pp. 2367–2378.

[4] Mukawa, S. Effect of $CaF_2$ addition, temperature, basicity and lime diameter on the rate of hot metal dephosphorization. *Tetsu-to-Hagane*, Vol. 100, 2014, pp. 509–515.

[5] Diao, J. Effect of $Al_2O_3$ and $Na_2O$ on dephosphorization of high phosphorus hot metal. *Journal of Iron and Steel Research*, Vol. 25, 2013, pp. 9–13 (in Chinese).

[6] Pak, J. J., and R. J. Fruehan. The effect of $Na_2O$ on dephosphorization by CaO-based steelmaking slags. *Metallurgical and Materials Transactions B*, Vol. 22, 1991, pp. 39–46.

[7] Jung, I. H., J. D. Seo, and S. H. Kim. Thermodynamic behaviours of manganese and phosphorus between CaO–MgOsat–$SiO_2$–$Al_2O_3$–FetO–MnO–$P_2O_5$ ladle slag and liquid iron. *Steel Research International*, Vol. 71, 2000, pp. 333–339.

[8] Gao, X., H. Matsuura, M. Miyata, and F. Tsukihashi. Phase equilibrium for the CaO–$SiO_2$–FeO–5mass%$P_2O_5$–5mass%$Al_2O_3$ system for dephosphorization of hot metal pretreatment. *ISIJ International*, Vol. 53, 2013, pp. 1381–1385.

[9] Gao, X., Matsuura, H., I. Sohn, W. L. Wang, D. J. Min, and F. Tsukihashi. Phase relationship for the CaO–$SiO_2$–FeO–5mass%$P_2O_5$ system with oxygen partial pressure of $10^{-8}$ atm at 1673 and 1623K. *Materials Transactions*, Vol. 54, 2013, pp. 544–552.

[10] Shu, Q. F., and K. C. Chou. Calculation for density of molten slags using optical basicity. *Ironmaking and Steelmaking*, Vol. 40, 2013, pp. 571–577.

[11] Ray, H. S., and S. Pal. Simple method for theoretical estimation of viscosity of oxide melts using optical basicity. *Ironmaking and Steelmaking*, Vol. 31, 2004, pp. 125–130.

[12] Duffy, J. A. Polarisability and polarising power of rare earth ions in glass: an optical basicity assessment. *Physics and Chemistry of Glasses*, Vol. 46, 2005, pp. 1–6.

[13] Zhao, X. Y., X. L. Wang, H. Lin, and Z. Q. Wang. Electronic polarizability and optical basicity of lanthanide oxides. *Physica B: Condensed Matter*, Vol. 392, 2007, pp. 132–136.

[14] Xi, X. J., S. F. Yang, J. S. Li, D. Q. Luo, X. N. Cai, and C. B. Lai. Phosphorus distribution between rare earth oxides containing slags and ferromanganese alloy. *Ironmaking and Steelmaking*, Vol. 46, 2019, pp. 485–490.

[15] Wang, D. Y. Effect of rare earth and its oxides on the chemical and physical properties of mold flux for continuous casting. PhD dissertation. Northeastern University, Shenyang, 2004 (in Chinese).

[16] Xi, X. J., S. F. Yang, C. B. Lai, J. S. Li, and F. Wang. Thermal physical properties and dephosphorisation kinetics of rare earth oxides containing slags. *Ironmaking and Steelmaking*, Vol. 46, 2019, pp. 968–973.

[17] Wu, C. C. Research on the rare earth addition technology and theory in refining process for special steel. PhD dissertation. University of Science and Technology Beijing, Beijing, 2014 (in Chinese).

[18] Chaudhary, P. N., R. P. Goel, and G. G. Roy. Dephosphorisation of high carbon ferromanganese using $BaCO_3$ based fluxes. *Ironmaking and Steelmaking*, Vol. 28, 2001, pp. 396–403.

[19] Xi, X. J. Development of rare earth oxide containing slags for oxidative dephosphorization of ferromanganese. PhD dissertation. Jiangxi University of Science and Technology, Ganzhou, 2017 (in Chinese).

[20] Tong, Z. F., J. L. Qiao, and X. Y. Jiang. Hot metal desulfurization kinetics by CaO–$Al_2O_3$–$SiO_2$–MgO–$TiO_2$–$Na_2O$ slags. *ISIJ International*, Vol. 57, 2017, pp. 245–253.

[21] Zuo, H. B., C. Wang, C. F. Xu, J. L. Zhang, and T. Zhang. Effects of MnO on slag viscosity and wetting behaviour between slag and refractory. *Ironmaking and Steelmaking*, Vol. 43, 2016, pp. 56–63.

[22] Xi, X. J., C. B. Lai, L. Gan, Z. H. Deng, Y. L. Peng, and Z. M. Zhang. Melting properties and viscosity of ferromanganese dephosphorization slag containing $Ce_2O_3$. *Iron Steel*, Vol. 51, 2016, pp. 26–29 (in Chinese).

[23] Yang, Y. D., A. R. McKague, A. McLean, and I. D. Sommerville. Dephosphorization thermodynamics of crude steel using CaO-based flux. *Journal of Iron and Steel Research International*, Vol. 10, 2003, pp. 10–15.